ACS Photonics

Article

pubs.acs.org/journal/apchd5

Dynamical Instability of a Nonequilibrium Exciton-Polariton Condensate

Nataliya Bobrovska,*[,†] Michał Matuszewski,[†] Konstantinos S. Daskalakis,[‡] Stefan A. Maier,[§] and Stéphane Kéna-Cohen[∥]

[†]Institute of Physics, Polish Academy of Sciences, Al. Lotników 32/46, 02-668 Warsaw, Poland

[‡]COMP Centre of Excellence, Department of Applied Physics, Aalto University, PO Box 15100, Fi-00076 Aalto, Finland

[§]Department of Physics, Imperial College London, London SW7 2AZ, United Kingdom

[∥]Department of Engineering Physics, Polytechnique Montréal, Montréal, Québec H3C 3A7, Canada

Supporting Information

ABSTRACT: By imaging single-shot realizations of an organic polariton quantum fluid, we observe the long-sought dynamical instability of nonequilibrium condensates. We find an excellent agreement between the experimental data and a numerical simulation of the open-dissipative Gross-Pitaevskii equation, without performing any parameter fitting, which allows us to draw several important conclusions about the physics of the system. We find that the reservoir dynamics are in the strongly nonadiabatic regime, which renders the complex Ginzburg−Landau description invalid. The observed transition from stable to unstable fluid can only be explained by taking into account the specific form of reservoir-mediated instability as well as particle currents induced by the finite extent of the pump spot.

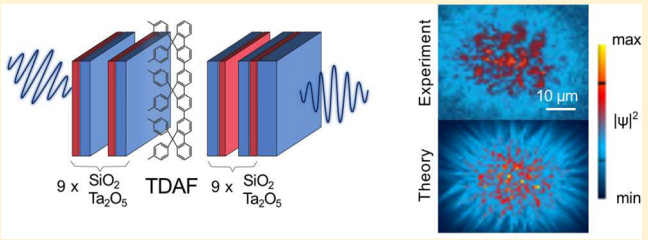

KEYWORDS: *exciton-polariton, Bose−Einstein condensation, organic condensate, dynamical instability*

Semiconductor microcavities are one of the most versatile systems for realizing and studying quantum fluids of light.[1] As a result of the strong coupling between light and matter modes at resonance, new excitations called exciton-polaritons are formed. These hybrid quasiparticles are coherent superpositions of the semiconductor exciton and microcavity photon, which can inherit properties derived from both fundamental constituents.[2−4] Although their low effective mass has been touted as an advantage for realizing equilibrium polariton condensates, the driven-dissipative nature of polariton systems, a result of the short particle lifetime, plays an important role in the condensation process. Indeed, the vast majority of experiments are performed in conditions where the polariton gas is out of equilibrium. Still, this allows for several phenomena related to Bose−Einstein condensation to be observed at temperatures much higher than those required for cold atom systems,[5−7] while also stimulating new questions.[8] In addition to fundamental research, the physics of nonequilibrium polariton condensates is attractive for its potential applications. Polariton condensates are intrinsically low-threshold sources of coherent light[9,10] and polariton devices have been used as interferometers[11] and polariton circuit elements.[12−14] Moreover, nonlinearities due to strong exciton-mediated interactions give rise to fascinating physical properties such as superfluidity,[15,16] black hole physics,[17] and solitons.[18,19] Recently, such nonlinearities have also been demonstrated in organic semiconductors,[20−22] which is attractive for the realization of room-temperature devices.

Despite these remarkable developments, the physics of nonresonantly pumped polariton condensates is still not completely understood. Condensation requires external optical[5] or electronic[10,23] pumping, which creates a reservoir of high-energy electronic excitations. The energetic relaxation of these excitations due to interaction with the environment enhanced by bosonic stimulation can then lead to a macroscopic occupation of the low-lying polariton ground state. This complicated process has been modeled theoretically within various approximations.[24−29] A particularly useful description is based on the phenomenological open-dissipative Gross-Pitaevskii equation (ODGPE).[30] Its application is widespread due to the simplicity of this description, the limited number of free parameters required, and its success in reproducing experimental results. We note that a similar model was also used to describe nonequilibrium condensates in atom laser systems.[31]

Since the introduction of the ODGPE model,[30] it was realized that for certain parameters it predicts a peculiar instability of the condensate due to the interaction of polaritons

Special Issue: Strong Coupling of Molecules to Cavities

Received: March 21, 2017
Published: August 10, 2017

DOI: 10.1021/acsphotonics.7b00283
ACS Photonics 2018, 5, 111−118

with the reservoir of uncondensed excitons. This dynamical instability is due to the repulsive interaction of condensed polaritons with reservoir excitons, and is excpected to result in phase separation of the two components. Since to date there was no experimental evidence of this instability, its physical relevance was unclear. Some authors have suggested that the instability is an artifact that would disappear when energy relaxation in the condensate was properly accounted for.[26,32,33] Many theoretical studies circumvented this problem by imposing the adiabatic assumption of a fast reservoir response, either indirectly by choosing a reservoir lifetime much shorter than the typical lifetime of an exciton or directly by using a simplified complex Ginzburg–Landau (CGLE) description with no separate reservoir degree of freedom.[34,35] In this regime, the model becomes instability free.[36]

Here, we demonstrate that the reservoir-induced instability is a real phenomenon that can occur in nonequilibrium polariton condensates. We confirm this by measuring single-shot realizations of the condensate emission from an oligofluorene-filled organic microcavity. The results are compared to the predictions of the ODGPE model without any parameter fitting, as all the parameters were determined in an independent study on the same sample.[22] Previous measurements of first-order spatial correlations in this system hinted at the possible breakdown of the stable condensate model.[37] Excellent agreement between experiment and numerical modeling allows us to determine that the lifetime of the reservoir indeed places the system in the unstable and strongly nonadiabatic regime, where the simplified CGLE-like description does not provide a reliable description of system dynamics. We also demonstrate that there is a transition from a stable to an unstable condensate with increasing pump power. This behavior is in opposition with the previously reported stability criterion obtained for continuous wave pumping.[38] We explain this seeming contradiction as resulting from a competition between reservoir-induced instability, finite condensate lifetime under pulsed excitation, and stabilizing effect of particle currents. Although the experiment we describe was performed on an organic microcavity, the ODGPE model we use to interpret the results holds equally well for inorganics (neglecting the spin degree of freedom). We conclude by discussing the relevance of our findings to the stability and coherence of inorganic polariton condensates.

MODEL

We model the exciton-polariton condensate using the two-dimensional stochastic ODGPE for the wave function $\psi(\mathbf{r},t)$ coupled to the rate equation for the polariton reservoir density, $n_R(\mathbf{r},t)$[25,30]

$$i\mathrm{d}\psi = \left[-\frac{\hbar}{2m^*}\nabla^2 + \frac{g_C}{\hbar}|\psi|^2 + \frac{g_R}{\hbar}n_R + V(\mathbf{r}) + \frac{i}{2}(Rn_R - \gamma_C)\right]\psi\,\mathrm{d}t + \mathrm{d}W \quad (1)$$

$$\frac{\partial n_R}{\partial t} = P - (\gamma_R + R|\psi|^2)n_R - k_b n_R^2 \quad (2)$$

where $P(\mathbf{r},t)$ is the exciton creation rate due to the pumping pulse, m^* is the effective mass of lower polaritons, γ_C and γ_R are the polariton and exciton dissipation rates, R is the rate of stimulated scattering to the condensate, g_C and g_R are the polariton–polariton and polariton–reservoir interaction coefficients, respectively, and k_b is the bimolecular annihilation rate. The latter is specific property of organic semiconductors, but it does not qualitatively affect the calculation results. With the exception of the pumping and dissipation terms, eq 1 is analogous to the Gross-Pitaevskii equation used to describe atomic condensates, where g_C plays the role of a contact interaction. The quantum noise $\mathrm{d}W$ can be obtained within the truncated Wigner approximation[25] as Gaussian noise with correlations $\langle \mathrm{d}W(\mathbf{r})\mathrm{d}W^*(\mathbf{r}')\rangle = \frac{\mathrm{d}t}{2(\Delta x)^2}(Rn_R + \gamma_C)\delta_{\mathbf{r},\mathbf{r}'}$ and $\langle \mathrm{d}W(\mathbf{r})\mathrm{d}W(\mathbf{r}')\rangle = 0$, where Δx is the lattice constant of the discretized mesh. In eq 2, we assume that the pump pulse length (τ_{pulse} = 250 fs) is short enough that $P(\mathbf{r},t)$ as a $\delta(t)$ function in time. In most calculations, we neglect the effect of static disorder of the sample $V(\mathbf{r})$. This assumption will be justified by comparison with experimental data in Figure 4. All of the model parameters were previously obtained from the power dependence and blueshift.[22,37] They are summarized in Figure 2.

The cavity under consideration is shown schematically in Figure 1 and composed of a single thin film of 2,7-bis[9,9-di(4-methylphenyl)-fluoren-2-yl]-9,9-di(4-methylphenyl)fluorene (TDAF) sandwiched between two dielectric Bragg mirrors composed 9 pairs of alternating Ta_2O_5/SiO_2. The sample fabrication was previously described in ref 22. Samples were fabricated on quartz substrates and excitation and detection were performed in a transmission geometry. The pulsed excitation was provided by an optical parametric amplifier (Orpheus, Light Conversion) pumped by an Yb:KGW amplifier operating at 100 Hz (PHAROS, Light Conversion). The slow repetition rate allowed sufficient time for the CCD camera (Thorlabs BC106-VIS) to capture each frame within the read time.

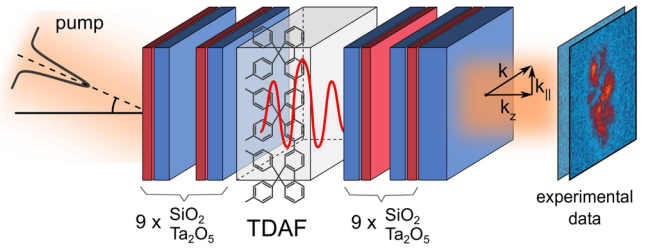

Figure 1. Schematic of the sample, which is composed of an amorphous oligofluorene film sandwiched between two dielectric Bragg mirrors. A high energy impulsive pump was incident on the sample at a θ = 50° angle. The near-field images, representatively shown on the right, were obtained by collecting the photoluminescence on a CCD camera.

INSTABILITY OF THE CONDENSATE

As previously reported, the condensate solution is prone to dynamical instabilities for a certain range of parameters.[30] The physical origin of this instability is the repulsive interaction g_R between the condensate and reservoir excitons, which can lead to phase separation of these two components. For the parameters of our system, the instability is predicted to occur for all continuous pump powers below $P = (g_R\gamma_C)/(g_C\gamma_R)P_{th} \approx 3000P_{th}$.[38] This greatly exceeds the range of pump powers accessible here and in any other organic microcavity for typical values γ_C and γ_R.[39] Many inorganic microcavities also fall within the instability regime.

DOI: 10.1021/acsphotonics.7b00283
ACS Photonics 2018, 5, 111–118

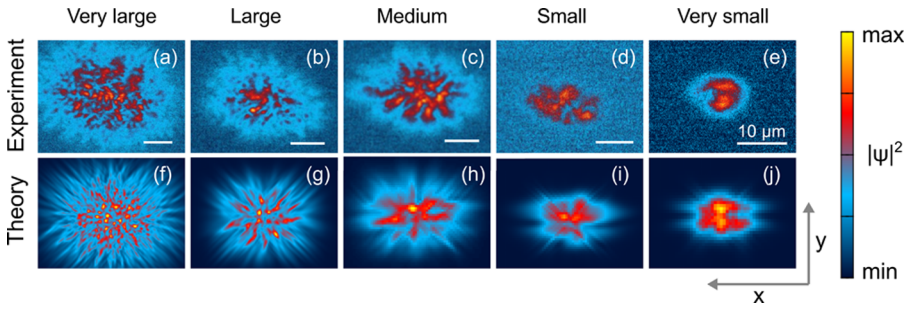

Figure 2. Comparison between the time-integrated experimental (top) and numerical (bottom) polariton field density. The size of the pump spot decreases from (a), (f) to (e), (j). The instability leads to the creation of polariton domains. The color scale is normalized to maximum value in each frame separately. Parameters used in numerical simulations are $m^* = 2.1 \times 10^{-5} m_e$, $R = 1.1 \times 10^{-2}$ cm^2 s^{-1}, $\gamma_C = (167$ fs$)^{-1}$, $\gamma_R = (300$ ps$)^{-1}$, $g_C = 10^{-6}$ meV μm^2, $g_R = 1.7 \times 10^{-6}$ meV μm^2, $k_b = 3.3 \times 10^{-5}$ cm^2 s^{-1} and correspond to the values measured in ref 22.

Single-shot real space images of the condensate photoluminescence are shown in Figure 2a–e for varying dimensions of the Gaussian pump. These were taken at a pump power $P = 2P_{th}$ for Figure 2a–d and $P = 2.5P_{th}$ for Figure 2e, where P_{th} is the condensation threshold. The corresponding ODGPE calculations for the same powers, where only the shape of the pump is varied are shown below in Figure 2f–j. The agreement is remarkable given that no parameter fitting was applied. The experiment and calculation highlight that the instability is more pronounced for large spatial pump sizes (or flat-top, which is not shown). In contrast, the smallest condensate size is only slightly affected by the instability.

Note that both the experiment and the calculation are time-averaged over the duration of the condensate emission for each pulse. The exact size and orientation of the patterns varies randomly from shot to shot, both in experiment and simulations, but these remain qualitatively the same. In Figure 3 we show examples of single-shot luminescence patterns coming from the same point on the sample. The experimental results (a) are compared with numerical results in two cases: the unstable regime of parameters, as in Figure 2, and stable regime with the addition of a disorder $V(\mathbf{r})$ (b). The stable regime was obtained here by the reduction of the pump power (cf. Figure 8). The disorder amplitude was chosen to be large enough so that its presence can induce the creation of polariton domains similar as in the experiment, and its correlation length was tuned to the typical domain size. Clearly, the disorder-induced domains in the stable regime (c) are placed in the same positions from shot to shot, while both in experiments and simulations (b) their placement is random. This effect leads to the observed smearing out of the domain patterns when averaging over multiple shots, observed both in the experiment and in the simulations. This suggests that disorder does not play an important role in determining the final condensate profile. This is in contrast to previous works, where polariton domains were observed in luminescence averaged over a long time or multiple shots (e.g., refs 5, 40, and 41), pointing out that their position was fixed by local disorder fluctuations.

To further verify this assumption quantitatively, we measured the shot-to-shot variations of the luminescence intensity from several points on the sample. The experimental results are compared on Figure 4 with numerical results in two cases: the unstable regime of parameters, and the stable regime with the addition of a static disorder potential $V(\mathbf{r})$. The variation of intensity at each of the points is in the latter case much lower than observed experimentally, due to pinning of domains to the potential minima. This allows to discard the hyphotesis that

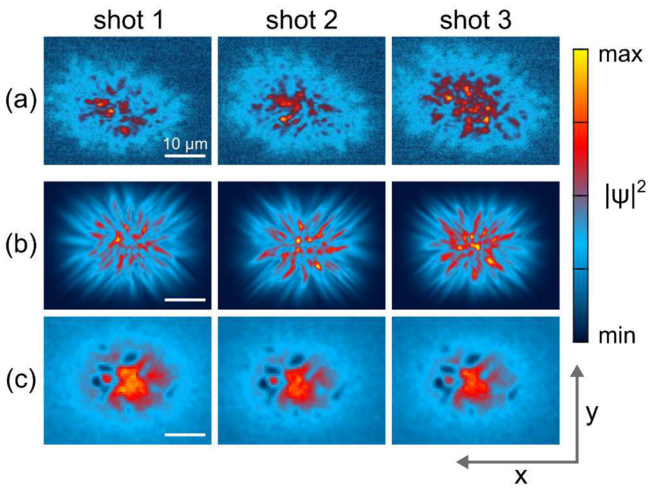

Figure 3. Examples of single-shot luminescence patterns from (a) experiments, (b) numerical simulations in the unstable regime, and (c) numerical simulations in the stable regime, where the polariton domains are created by disorder. The size of the pump corresponds to the "Large" spot, and other parameters are as in Figure 2.

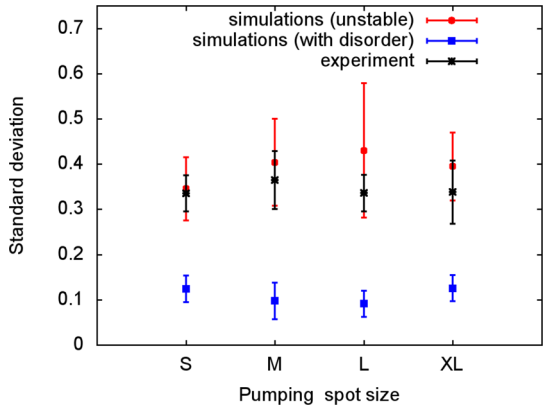

Figure 4. Effect of sample disorder. Normalized standard deviation of shot-to-shot local luminescence $\sigma[I(\mathbf{r}_0)]/\langle I(\mathbf{r}_0)\rangle$, as measured in the experiment and predicted by the model in the unstable regime and in the stable regime with the addition of static disorder (40 shots in each case). The disorder amplitude was chosen to be large enough so that its presence can induce the creation of polariton domains, similar as in the experiment, and its correlation length was tuned to the typical domain size. The error bars are obtained by averaging over five different points on the sample $\mathbf{r}_0$.

DOI: 10.1021/acsphotonics.7b00283
ACS Photonics 2018, 5, 111–118

domains are created in a stable condensate solely due to the effect of disorder.

The excellent agreement between the experiment and theory allows us to draw some important conclusions about the physics of the system. The parameters of the model indicate that the dynamics are not only in the unstable, but also strongly nonadiabatic regime, that is, the reservoir $n_R(\mathbf{r},t)$ does not quickly follow the changes in the condensate density $|\psi(\mathbf{r},t)|^2$. The adiabatic regime is attained only when three independent analytical conditions are fulfilled simultaneously (see Supporting Information). Here, all three conditions are violated. In particular, $g_R n_R \approx 40(\gamma_R + R|\psi|^2)$, which means that the reaction time of the reservoir is 40× slower than the response time of the condensate due to interactions with the reservoir.

The breakdown of the adiabatic approximation suggests that CGLE-like models based on a single equation cannot reliably describe the dynamics of the system. This is due to the fact that they do not not incorporate the reservoir as a separate degree of freedom. We demonstrate this by numerically modeling the single stochastic Gross-Pitaevskii equation (SGPE)[33,42] for the same parameters. As shown in Figure 5a, this model gives a poor agreement to the experimental data. The coefficients of the SGPE equation were determined using the correspondence formulas derived in ref 36. The effective interaction between polaritons turns out to be attractive, which is due to the reservoir-mediated attraction in the unstable regime. Nevertheless, the instability does not give rise to multiple domains, but rather to condensate collapse with no spatial symmetry breaking. We also verified that SGPE simulations with an explicit repulsive interaction coefficient are not able to reproduce the experimental patterns, see Figure 5b. The details of the model are given in the Supporting Information.

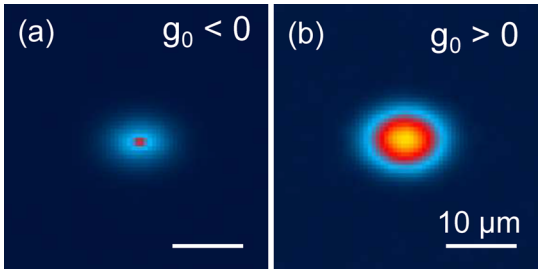

Figure 5. Results of numerical simulations using the CGLE-based stochastic Gross-Pitaevskii equation. Parameters correspond to the very small spot (e) case from Figure 2 (see text).

TRANSITION FROM STABLE TO UNSTABLE CONDENSATE

For a large size of the pump spot, we generally observe the instability independently of the pump pulse power, see Figure 2. However, in the case of a small size (e.g., Figure 2e,j, a transition from a stable to an unstable condensate is seen with increasing pump power (see Figure 6). When the power of the pump pulse is less than about $1.8P_{th}$, a single condensate is formed, while for pump powers above this value, the instability results in the appearance of two or more domains. Note that this stable region is precisely where first-order spatial coherence measurements were previously reported. Stability is a necessity due the extraction procedure, which requires fitting several interferograms as a function of phase delay. Any shot-to-shot fluctuations consequently lead to an artificial reduction of the fringe visibility. Finally, via numerical simulations, we observe that the transition from stable to unstable is not abrupt and that there is some shot-to-shot variation along the boundary.

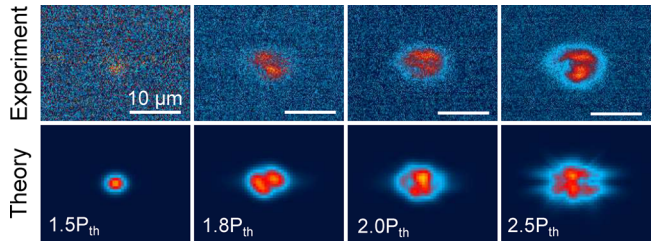

Figure 6. Comparison between the time-integrated experiment (top) and numerical (bottom) polariton field density obtained for the very small Gaussian pumping spot for different pump powers.

The observed power dependence is in contradiction with the previously predicted transition from an unstable to a stable condensate with increasing continuous wave pumping.[38,43] To understand this effect, we developed a theoretical model of condensation dynamics under impulsive excitation. The main elements that determine the stability of the condensate are the unstable dynamical Bogoliubov spectrum of the condensate, the density current of polaritons flowing away from the center of the pumping spot, and the finite lifetime of the condensate. The competition of these processes can explain the existence of stable or unstable condensate for various pumping conditions and allows for the calculation of the transition region.

The evolution of the system can be divided into several stages shown in Figure 7a–c. At the arrival of the ultrashort pulse, the reservoir density is fixed according to the Gaussian profile of the pump, while the wave function ψ contains only random fluctuations inherited from the Wigner noise. Due to the finite size of the pump spot, a polariton current from the center of the pump spot is created by the reservoir-induced potential. This favors the formation of a single condensate, as the most central fluctuation "spills over" and repels the other domains outside. However, for large pumping powers a single condensate is not formed, and the system evolves to a fragmented state, while some flow of polaritons from the center is still visible. We attribute this effect to the existence of unstable Bogoliubov modes which break up the condensate. These unstable modes are always present, but for low pumping powers, the instability is too weak to develop during the lifetime of the condensate. The condensate lifetime is understood here as the full width at half-maximum duration of the emission from the condensate, see Figure 7.

To quantify this, we have calculated the Bogoliubov instability time scale in the local-density approximation, that is, neglecting the spatial inhomogeneity of the pump. We find that, in the case of a pulsed pump, the dynamical Bogoliubov spectrum can be qualitatively different from the one in the case of continuous pumping, which was considered in previous reports,[30,38,44,45] due to the absence of the pumping term after the arrival of the pulse (see below). For our parameters, the resulting imaginary part of the unstable Bogoliubov branch frequency is shown in Figure 7(iii) and is inversely related to the instability time scale.

Instead of examining stability about a steady-state, we consider small fluctuations around the homogeneous state with a polariton and reservoir density evolving in time

DOI: 10.1021/acsphotonics.7b00283
ACS Photonics 2018, 5, 111–118

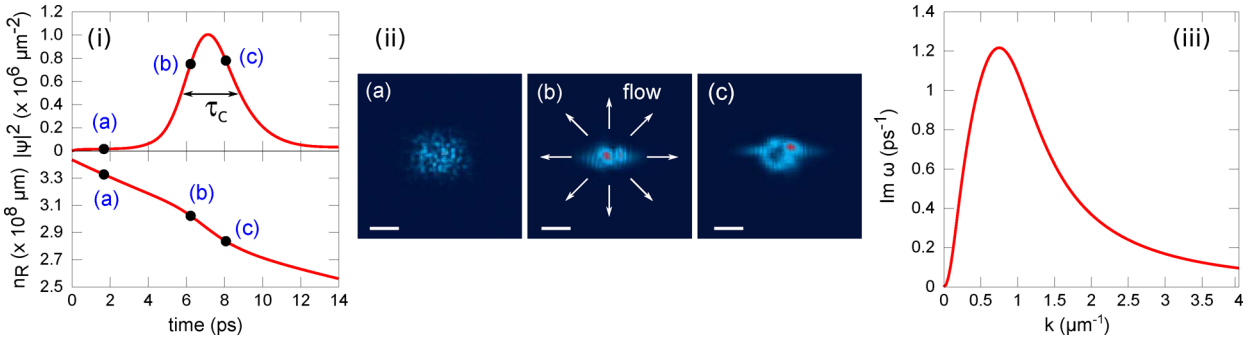

Figure 7. Development of the condenste instability for the small Gaussian spot at power $P = 1.6P_{th}$. The left panel (i) shows the simulated evolution of the condensate and reservoir particle number, with the condensate lifetime τ_C defined as the fwhm duration of the condensate emission. Panel (ii) with frames (a)−(c) shows snapshots of density profiles at the three chosen instants of time. The outgoing flow of polaritons is responsible for the creation of a single condensate. At high pumping, the Bogoliubov instability breaks up the condensate, as shown in frames (b) and (c). (iii) Imaginary part of the frequency of the unstable Bogoliubov branch calculated with eq 4 at peak polariton density.

$$\psi = \psi_0 e^{-i\mu t/\hbar + \beta_C t/2}\left(1 + \sum_{\mathbf{k}} \left[u_{\mathbf{k}} e^{-i(\omega_{\mathbf{k}} t - \mathbf{kr})} + v_{\mathbf{k}}^* e^{i(\omega_{\mathbf{k}}^* t - \mathbf{kr})}\right]\right),$$
$$n_R = n_R^0 e^{\beta_R t}\left(1 + \sum_{\mathbf{k}} \left[w_{\mathbf{k}} e^{-i(\omega_{\mathbf{k}} t - \mathbf{kr})} + \text{c. c.}\right]\right) \quad (3)$$

where $\omega_{\mathbf{k}}$ is the frequency of the mode with the wavenumber $\mathbf{k}$, and $u_{\mathbf{k}}$, $v_{\mathbf{k}}$, and $w_{\mathbf{k}}$ are small fluctuations. In the above $\beta_{C,R}$ are condensate and reservoir density growth or decay rates that need to be taken into account in the case of pulsed excitation.

Consider a condensate and reservoir that are approximately spatially homogeneous (as in the standard Bogoliubov method) but with the average densities increasing or decreasing in time due to imbalance in loss and gain. Small spatial fluctuations on top of this state may grow or decay independently of the growth or decay of the average condensate or reservoir density. For example, while the average condensate density grows from t_1 to t_2 by 10%, the fluctuations of the wave function in space may grow from 1% of the average amplitude at t_1 to 2% of average amplitude at t_2, that is, the condensate wave function may become more "rough". When t_1 and t_2 differ by an infinitesimally small amount dt, we can calculate the instantaneous growth rate of these fluctuations analytically. In practice, we can calculate the complex frequency of these fluctuations.

The growth rates calculated in this way are time-dependent, since the state of the condensate and reservoir change in time. After long time of evolution, growth (or decay) of a fluctuation will be given by its instantaneous growth rate integrated over time. We note that we treat the condensate and reservoir (both the homogeneous base states and fluctuations around them) as separate degrees of freedom; therefore, the calculation is not limited to the adiabatic approximation. The resulting fluctuation eigenmodes are appropriate combinations of condensate and reservoir fluctuations.

The excitation spectrum is described by the eigenvalue problem $\mathcal{L}_{\mathbf{k}}\mathcal{U}_{\mathbf{k}} = \hbar\omega_{\mathbf{k}}\mathcal{U}_{\mathbf{k}}$, where $\mathcal{U}_{\mathbf{k}} = (u_{\mathbf{k}}, v_{\mathbf{k}}, w_{\mathbf{k}})^T$ and

$$\mathcal{L}_{\mathbf{k}} = \begin{pmatrix} g_C n_p + \epsilon_k & g_C n_p & \left(\frac{i\hbar}{2}R + g_R\right)n_R^0 \\ -g_C n_p & -g_C n_p - \epsilon_k & \left(\frac{i\hbar}{2}R - g_R\right)n_R^0 \\ -i\hbar R n_p & -i\hbar R n_p & -i\hbar(P/n_R^0 + k_b n_R^0) \end{pmatrix} \quad (4)$$

and $\epsilon_k = \hbar^2k^2/2m^*$, $n_p = |\psi_0|^2$, $\mu = n_p g_C + g_R n_R^0$, $\beta_C = Rn_R^0 - \gamma_C$, $\beta_R = P/n_R^0 - n_p R - \gamma_R$. In the special case of a stationary state under CW (continuous wave) pumping the above matrix is equivalent to the one considered before.[30]

In the pulsed case, we have $P = 0$ after the arrival of the pulse and, consequently, $\beta_R < 0$, that is, the decay of the reservoir density. It is easy to see that the matrix (eq 4) has then a qualitatively different form, and the calculated spectrum differs substantially from the CW case.

The Bogoliubov instability time τ_B is calculated from the Bogoliubov spectrum taking the polariton density equal to half of the maximum density (corresponding to the spatial average with a Gaussian shape of the condensate) times one-half due to the temporal dependence of the density as in Figure 7. For consistency, the condensate lifetime is taken as the full width at half-maximum of the temporal dependence of the density. The instability time scale is estimated as $tau_B = 2.5/\max_k(\text{Im}\omega_k)$, where we assume that initial density fluctuations on the level of 8% of the maximum density can develop into domains. These fluctuations are not mainly seeded by the Wigner noise, which are rather small, but by the inhomogeneous shape of the reservoir. The value of 8% fluctuation is consistent with the spatial variation of the initial reservoir density on the area where the condensate is typically formed.

We emphasize that the flow of polaritons explains the formation of a single domain from initial noise at low pumping powers, as follows from analysis of numerical simulations. This process is a linear effect, independent of the density, so it is not limited by the lifetime of the high-density condensate, but by the time of the formation of the condensate. For this reason, it dominates at low pumping powers.

A comparison between the Bogoliubov instability time scale and the condensate lifetime is shown in Figure 8. We find that the Bogoliubov time scale τ_B is longer than the condensate lifetime τ_C for $n_0/n_{th} \lesssim 1.8$, where n_0 is the maximum of $n_R(\mathbf{r},t = 0)$ and n_{th} is the threshold value of n_0 for condensate formation,

DOI: 10.1021/acsphotonics.7b00283
ACS Photonics 2018, 5, 111−118

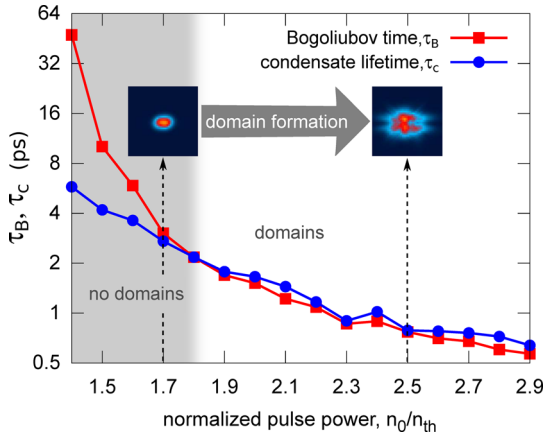

Figure 8. Comparison between the characteristic time scales that are responsible for the development of the instability. According to numerical simulations, polariton domains are formed only when the Bogoliubov instability time τ_B becomes comparable to the lifetime of the condensate emission τ_C, which is determined as in Figure 7. At lower density, a single symmetric condensate is created. Averaged over five realizations.

see Figure 8. Above this value, these time scales become comparable. This is in very good agreement with the observed threshold for domain formation, see Figure 6. The similarity between the time scales τ_B and τ_C above $n_0/n_{th} \approx 1.8$ is explained by the similar magnitude of all nonlinear coefficients ($\hbar R$, g_C, and g_R) in eq 1. At high pump powers, the maximum density of the condensate $|\psi|^2$ becomes comparable to n_R, and all nonlinear energy scales have similar order of magnitude; in particular, the spontaneous scattering rate $R|\psi|^2$, which depletes the reservoir and influences the lifetime.

RELEVANCE TO INORGANIC CONDENSATES

The vast majority of exciton-polariton condensates are realized in inorganic semiconductors, where properties are slightly different from the organic case considered here. Nevertheless, the parameters of inorganic samples also place them in the unstable regime. In particular, independent measurements[46] as well as modeling of dynamics[47−49] indicate a reservoir lifetime in the hundreds of picoseconds, which suggests that it should not be treated adiabatically. In several experiments, however, the "bottleneck" region plays the role of the reservoir, and the relaxation kinetics may need to be considered. In contrast, organic microcavities have short enough polariton lifetimes that single-step relaxation processes from the reservoir can be considered to be dominant. Meanwhile, instabilities in inorganic condensates may be present in some systems, but obscured, because of the absence of single-shot measurements. The difficulty in performing such measurements is mostly due to the lower polariton densities typical of inorganic microcavities. In our samples, averaging over tens of pulses already wash out clear signatures of the domain formation. An alternative to single-shot experiments is the measurement of spatial correlation functions in which the signatures of domains can persist. Indeed, this is observed in the microcavity considered here as a reduction in the first-order spatial coherence.[37]

CONCLUSIONS

In conclusion, we have demonstrated for the first time the reservoir-mediated instability of a nonequilibrium exciton-polariton condensate. Excellent agreement between the experiment and the theory suggests that models with reservoir treated as a separate degree of freedom should be used to describe these systems. Under pulsed excitation, we find that various time scales determine that stability limit, including the finite condensate duration, the reservoir-induced instability, and particle currents due to repulsive exciton−polariton interactions.

ASSOCIATED CONTENT

Supporting Information

The Supporting Information is available free of charge on the ACS Publications website at DOI: 10.1021/acsphotonics.7b00283.

Section S1: Adiabaticity conditions; Section S2: The role of polariton-polariton interactions; Section S3: Simplified Stochastic Gross-Pitaevskii equation; Section S4: The effect of quantum noise (PDF).

AUTHOR INFORMATION

Corresponding Author

*E-mail: nbobrov@ifpan.edu.pl.

ORCID

Nataliya Bobrovska: 0000-0003-0084-0213
Michał Matuszewski: 0000-0001-8830-3302
Stéphane Kéna-Cohen: 0000-0001-5065-2750

Notes

The authors declare no competing financial interest.

ACKNOWLEDGMENTS

N.B. and M.M. acknowledge support from the National Science Center of Poland Grants DEC-2011/01/D/ST3/00482 and 2015/17/B/ST3/02273. S.K.C. acknowledges funding from the NSERC Discovery Grant program and Canada Research Chairs. S.A.M. acknowledges the EPSRC Active Plasmonics Programme EP/H000917/2, the Royal Society, and the Lee-Lucas Chair in Physics. K.S.D. acknowledges the Leverhulme Trust and EPSRC Active Plasmonics Programme and financial support by a Marie Skłodowska-Curie Action (H2020-MSCA-IF-2016, Project ID 745115).

REFERENCES

(1) Carusotto, I.; Ciuti, C. Quantum fluids of light. *Rev. Mod. Phys.* **2013**, *85*, 299−366.
(2) Hopfield, J. J. Theory of the Contribution of Excitons to the Complex Dielectric Constant of Crystals. *Phys. Rev.* **1958**, *112*, 1555−1567.
(3) Weisbuch, C.; Nishioka, M.; Ishikawa, A.; Arakawa, Y. Observation of the coupled exciton-photon mode splitting in a semiconductor quantum microcavity. *Phys. Rev. Lett.* **1992**, *69*, 3314−3317.
(4) Kavokin, A.; Baumberg, J. J.; Malpuech, G.; Laussy, F. P. *Microcavities*; Oxford University Press, 2007.
(5) Kasprzak, J.; Richard, M.; Kundermann, S.; Baas, A.; Jeambrun, P.; Keeling, J. M. J.; Marchetti, F. M.; Szymańska, M. H.; André, R.; Staehli, J. L.; Savona, V.; Littlewood, P. B.; Deveaud, B.; Dang, L. S. Bose−Einstein condensation of exciton polaritons. *Nature* **2006**, *443*, 409−414.
(6) Roumpos, G.; Lohse, M.; Nitsche, W. H.; Keeling, J.; Szymańska, M. H.; Littlewood, P. B.; Löffler, A.; Höfling, S.; Worschech, L.; Forchel, A.; Yamamoto, Y. Power-law decay of the spatial correlation function in exciton-polariton condensates. *Proc. Natl. Acad. Sci. U. S. A.* **2012**, *109*, 6467−6472.

DOI: 10.1021/acsphotonics.7b00283
ACS Photonics 2018, 5, 111−118

(7) Byrnes, T.; Kim, N. Y.; Yamamoto, Y. Exciton-polariton condensates. *Nat. Phys.* **2014**, *10*, 803−813.
(8) Altman, E.; Sieberer, L. M.; Chen, L.; Diehl, S.; Toner, J. Two-Dimensional Superfluidity of Exciton Polaritons Requires Strong Anisotropy. *Phys. Rev. X* **2015**, *5*, 011017.
(9) Christopoulos, S.; von Högersthal, G. B. H.; Grundy, A. J. D.; Lagoudakis, P. G.; Kavokin, A. V.; Baumberg, J. J.; Christmann, G.; Butté, R.; Feltin, E.; Carlin, J.-F.; Grandjean, N. Room-Temperature Polariton Lasing in Semiconductor Microcavities. *Phys. Rev. Lett.* **2007**, *98*, 126405.
(10) Bhattacharya, P.; Frost, T.; Deshpande, S.; Baten, M. Z.; Hazari, A.; Das, A. Room Temperature Electrically Injected Polariton Laser. *Phys. Rev. Lett.* **2014**, *112*, 236802.
(11) Sturm, C.; Tanese, D.; Nguyen, H.; Flayac, H.; Galopin, E.; Lemaitre, A.; Amo, A.; Malpuech, G.; Bloch, J. All-optical phase modulation in a cavity-polariton Mach-Zehnder interferometer. *Nat. Commun.* **2014**, *5*, 3278.
(12) Amo, A.; Liew, T. C. H.; Adrados, C.; Houdré, R.; Giacobino, E.; Kavokin, A. V.; Bramati, A. Excitonpolariton spin switches. *Nat. Photonics* **2010**, *4*, 361−366.
(13) Gao, T.; Eldridge, P. S.; Liew, T. C. H.; Tsintzos, S. I.; Stavrinidis, G.; Deligeorgis, G.; Hatzopoulos, Z.; Savvidis, P. G. Polariton condensate transistor switch. *Phys. Rev. B: Condens. Matter Mater. Phys.* **2012**, *85*, 235102.
(14) Ballarini, D.; Giorgi, M. D.; Cancellieri, E.; Houdré, R.; Giacobino, E.; Cingolani, R.; Bramati, A.; Gigli, G.; Sanvitto, D. All-optical polariton transistor. *Nat. Commun.* **2013**, *4*, 1778.
(15) Amo, A.; Lefrére, J.; Pigeon, S.; Adrados, C.; Ciuti, C.; Carusotto, I.; Houdré, R.; Giacobino, E.; Bramati, A. Superfluidity of polaritons in semiconductor microcavities. *Nat. Phys.* **2009**, *5*, 805−810.
(16) Lagoudakis, K. G.; Wouters, M.; Richard, M.; Baas, A.; Carusotto, I.; André, R.; Dang, L. S.; Deveaud-Plédran, B. Quantized vortices in an exciton-polariton condensate. *Nat. Phys.* **2008**, *4*, 706−710.
(17) Nguyen, H. S.; Gerace, D.; Carusotto, I.; Sanvitto, D.; Galopin, E.; Lemaître, A.; Sagnes, I.; Bloch, J.; Amo, A. Acoustic Black Hole in a Stationary Hydrodynamic Flow of Microcavity Polaritons. *Phys. Rev. Lett.* **2015**, *114*, 036402.
(18) Amo, A.; Pigeon, S.; Sanvitto, D.; Sala, V. G.; Hivet, R.; Carusotto, I.; Pisanello, F.; Leménager, G.; Houdré, R.; Giacobino, E.; Ciuti, C.; Bramati, A. Polariton Superfluids Reveal Quantum Hydrodynamic Solitons. *Science* **2011**, *332*, 1167−1170.
(19) Sich, M.; Krizhanovskii, D. N.; Skolnick, M. S.; Gorbach, A. V.; Hartley, R.; Skryabin, D. V.; Cerda-Méndez, E. A.; Biermann, K.; Hey, R.; Santos, P. V. Observation of bright polariton solitons in a semiconductor microcavity. *Nat. Photonics* **2011**, *6*, 50−55.
(20) Kéna-Cohen, S.; Forrest, S. R. Room-temperature polariton lasing in an organic single-crystal microcavity. *Nat. Photonics* **2010**, *4*, 371−375.
(21) Plumhof, J. D.; Stöferle, T.; Mai, L.; Scherf, U.; Mahrt, R. F. Room-temperature Bose−Einstein condensation of cavity exciton-polaritons in a polymer. *Nat. Mater.* **2013**, *13*, 247−252.
(22) Daskalakis, K. S.; Maier, S. A.; Kena-Cohen, R. M. S. Nonlinear interactions in an organic polariton condensate. *Nat. Mater.* **2014**, *13*, 271−278.
(23) Schneider, C.; et al. An electrically pumped polariton laser. *Nature* **2013**, *497*, 348−352.
(24) Haug, H.; Doan, T. D.; Tran Thoai, D. B. Quantum kinetic derivation of the nonequilibrium Gross-Pitaevskii equation for nonresonant excitation of microcavity polaritons. *Phys. Rev. B: Condens. Matter Mater. Phys.* **2014**, *89*, 155302.
(25) Wouters, M.; Savona, V. Stochastic classical field model for polariton condensates. *Phys. Rev. B: Condens. Matter Mater. Phys.* **2009**, *79*, 165302.
(26) Solnyshkov, D. D.; Tercas, H.; Dini, K.; Malpuech, G. Hybrid Boltzmann-Gross-Pitaevskii theory of Bose−Einstein condensation and superfluidity in open driven-dissipative systems. *Phys. Rev. A: At., Mol., Opt. Phys.* **2014**, *89*, 033626.
(27) Laussy, F. P.; Malpuech, G.; Kavokin, A.; Bigenwald, P. Spontaneous Coherence Buildup in a Polariton Laser. *Phys. Rev. Lett.* **2004**, *93*, 016402.
(28) Galbiati, M.; Ferrier, L.; Solnyshkov, D. D.; Tanese, D.; Wertz, E.; Amo, A.; Abbarchi, M.; Senellart, P.; Sagnes, I.; Lemaître, A.; Galopin, E.; Malpuech, G.; Bloch, J. Polariton Condensation in Photonic Molecules. *Phys. Rev. Lett.* **2012**, *108*, 126403.
(29) Tassone, F.; Piermarocchi, C.; Savona, V.; Quattropani, A.; Schwendimann, P. Bottleneck effects in the relaxation and photo-luminescence of microcavity polaritons. *Phys. Rev. B: Condens. Matter Mater. Phys.* **1997**, *56*, 7554−7563.
(30) Wouters, M.; Carusotto, I. Excitations in a Nonequilibrium Bose−Einstein Condensate of Exciton Polaritons. *Phys. Rev. Lett.* **2007**, *99*, 140402.
(31) Kneer, B.; Wong, T.; Vogel, K.; Schleich, W. P.; Walls, D. F. Generic model of an atom laser. *Phys. Rev. A: At., Mol., Opt. Phys.* **1998**, *58*, 4841−4853.
(32) Wouters, M.; Liew, T. C. H.; Savona, V. Energy relaxation in one-dimensional polariton condensates. *Phys. Rev. B: Condens. Matter Mater. Phys.* **2010**, *82*, 245315.
(33) Chiocchetta, A.; Carusotto, I. Non-equilibrium quasi-condensates in reduced dimensions. *EPL* **2013**, *102*, 67007.
(34) Keeling, J.; Berloff, N. G. Spontaneous Rotating Vortex Lattices in a Pumped Decaying Condensate. *Phys. Rev. Lett.* **2008**, *100*, 250401.
(35) Sieberer, L. M.; Huber, S. D.; Altman, E.; Diehl, S. Dynamical Critical Phenomena in Driven-Dissipative Systems. *Phys. Rev. Lett.* **2013**, *110*, 195301.
(36) Bobrovska, N.; Matuszewski, M. Adiabatic approximation and fluctuations in exciton-polariton condensates. *Phys. Rev. B: Condens. Matter Mater. Phys.* **2015**, *92*, 035311.
(37) Daskalakis, K. S.; Maier, S. A.; Kéna-Cohen, S. Spatial Coherence and Stability in a Disordered Organic Polariton Condensate. *Phys. Rev. Lett.* **2015**, *115*, 035301.
(38) Smirnov, L. A.; Smirnova, D. A.; Ostrovskaya, E. A.; Kivshar, Y. S. Dynamics and stability of dark solitons in exciton-polariton condensates. *Phys. Rev. B: Condens. Matter Mater. Phys.* **2014**, *89*, 235310.
(39) Sanvitto, D.; Kéna-Cohen, S. The road towards polaritonic device. *Nat. Mater.* **2016**, *15*, 1061−1073.
(40) Lagoudakis, K. G.; Manni, F.; Pietka, B.; Wouters, M.; Liew, T. C. H.; Savona, V.; Kavokin, A. V.; André, R.; Deveaud-Plédran, B. Probing the Dynamics of Spontaneous Quantum Vortices in Polariton Superfluids. *Phys. Rev. Lett.* **2011**, *106*, 115301.
(41) Baas, A.; Lagoudakis, K. G.; Richard, M.; André, R.; Dang, L. S.; Deveaud-Plédran, B. Synchronized and Desynchronized Phases of Exciton-Polariton Condensates in the Presence of Disorder. *Phys. Rev. Lett.* **2008**, *100*, 170401.
(42) Gladilin, V. N.; Ji, K.; Wouters, M. Spatial coherence of weakly interacting one-dimensional nonequilibrium bosonic quantum fluids. *Phys. Rev. A: At., Mol., Opt. Phys.* **2014**, *90*, 023615.
(43) Liew, T. C. H.; Egorov, O. A.; Matuszewski, M.; Kyriienko, O.; Ma, X.; Ostrovskaya, E. A. Instability-induced formation and nonequilibrium dynamics of phase defects in polariton condensates. *Phys. Rev. B: Condens. Matter Mater. Phys.* **2015**, *91*, 085413.
(44) Byrnes, T.; Horikiri, T.; Ishida, N.; Fraser, M.; Yamamoto, Y. Negative Bogoliubov dispersion in exciton-polariton condensates. *Phys. Rev. B: Condens. Matter Mater. Phys.* **2012**, *85*, 075130.
(45) Bobrovska, N.; Ostrovskaya, E. A.; Matuszewski, M. Stability and spatial coherence of nonresonantly pumped exciton-polariton condensates. *Phys. Rev. B: Condens. Matter Mater. Phys.* **2014**, *90*, 205304.
(46) Bajoni, D.; Perrin, M.; Senellart, P.; Lemaître, A.; Sermage, B.; Bloch, J. Dynamics of microcavity polaritons in the presence of an electron gas. *Phys. Rev. B: Condens. Matter Mater. Phys.* **2006**, *73*, 205344.
(47) Wertz, E.; Amo, A.; Solnyshkov, D. D.; Ferrier, L.; Liew, T. C. H.; Sanvitto, D.; Senellart, P.; Sagnes, I.; Lemaître, A.; Kavokin, A. V.; Malpuech, G.; Bloch, J. Propagation and Amplification Dynamics of 1D Polariton Condensates. *Phys. Rev. Lett.* **2012**, *109*, 216404.

DOI: 10.1021/acsphotonics.7b00283
ACS Photonics 2018, 5, 111−118

(48) Gavrilov, S. S.; Brichkin, A. S.; Demenev, A. A.; Dorodnyy, A. A.; Novikov, S. I.; Kulakovskii, V. D.; Tikhodeev, S. G.; Gippius, N. A. Bistability and nonequilibrium transitions in the system of cavity polaritons under nanosecond-long resonant excitation. *Phys. Rev. B: Condens. Matter Mater. Phys.* **2012**, *85*, 075319.
(49) Lagoudakis, K. G.; Pietka, B.; Wouters, M.; André, R.; Deveaud-Plédran, B. Coherent Oscillations in an Exciton-Polariton Josephson Junction. *Phys. Rev. Lett.* **2010**, *105*, 120403.

DOI: 10.1021/acsphotonics.7b00283
ACS Photonics 2018, 5, 111−118